Protein-Doped Monolithic Silica Columns for Capillary Liquid Chromatography Prepared by the Sol–Gel Method: Applications to Frontal Affinity Chromatography

ARTICLE *in* ANALYTICAL CHEMISTRY · JUNE 2004

Impact Factor: 5.64 · DOI: 10.1021/ac0352124 · Source: PubMed

9 AUTHORS, INCLUDING:

Richard J Hodgson
University Health Network
19 PUBLICATIONS **433** CITATIONS
SEE PROFILE

Zheng Zhang
Semprus BioSciences
44 PUBLICATIONS **3,176** CITATIONS
SEE PROFILE

Anal. Chem. **2004,** *76,* 2780−2790

Protein-Doped Monolithic Silica Columns for Capillary Liquid Chromatography Prepared by the Sol−Gel Method: Applications to Frontal Affinity Chromatography

Richard J. Hodgson,[†,‡] Yang Chen,[†] Zheng Zhang,[†] Dina Tleugabulova,[†] Hong Long,[†] Xiaoming Zhao,[‡] Michael Organ,*[,‡] Michael A. Brook,*[,†] and John D. Brennan*[,†]

Department of Chemistry, McMaster University, Hamilton, Ontario, L8S 4M1, Canada, and Department of Chemistry, York University, Toronto, Ontario, M3J 1P3, Canada

The development of bioaffinity chromatography columns that are based on the entrapment of biomolecules within the pores of sol−gel-derived monolithic silica is reported. Monolithic nanoflow columns are formed by mixing the protein-compatible silica precursor diglycerylsilane with a buffered aqueous solution containing poly(ethylene oxide) (PEO, MW 10 000) and the protein of interest and then loading this mixture into a fused-silica capillary (150−250-μm i.d.). Spinodal decomposition of the PEO-doped sol into two distinct phases prior to the gelation of the silica results in a bimodal pore distribution that produces large macropores (>0.1 μm), to allow good flow of eluent with minimal back pressure, and mesopores (~3−5-nm diameter) that retain a significant fraction of the entrapped protein. Addition of low levels of (3-aminopropyl)triethoxysilane is shown to minimize non-selective interactions of analytes with the column material, resulting in a column that is able to retain small molecules by virtue of their interaction with the entrapped biomolecules. Such columns are shown to be suitable for pressure-driven liquid chromatography and can be operated at relatively high flow rates (up to 500 μL·min^{-1}) or with low back pressures (<100 psi) when used at flow rates of 5−10 μL·min^{-1}. The clinically relevant enzyme dihydrofolate reductase was entrapped within the bioaffinity columns and was used to screen mixtures of small molecules using frontal affinity chromatography with mass spectrometric detection. Inhibitors present in compound mixtures were retained via bioaffinity interactions, with the retention time being dependent on both the ligand concentration and the affinity of the ligand for the protein. The results suggest that such columns may find use in high-throughput screening of compound mixtures.

Bioaffinity chromatography has been widely used for sample purification and cleanup,[1] chiral separations,[2] on-line proteolytic digestion of proteins,[3] development of supported biocatalysts,[4] and more recently screening of compound libraries via the frontal affinity chromatography method.[5,6] In all cases, the predominant method used to prepare protein-loaded columns has been based on covalent or affinity coupling of proteins to solid supports. However, the coupling of proteins to beads has several limitations, including the following: loss of activity upon coupling (due to poor control over protein orientation and conformation), low surface area, potentially high back pressure (which may alter K_d values[7]), difficulty in the loading of beads into narrow-bore columns, difficulty in miniaturizing to very narrow columns (<50-μm i.d.), and poor versatility, particularly when membrane-bound proteins are used.[6]

A relatively recent advance in chromatographic columns is the development of monolithic stationary phases based on either

* To whom correspondence should be addressed. Tel: (905) 525-9140 (ext. 27033). Fax: (905) 522-2509. E-mail: brennanj@mcmaster.ca Internet: http://www.chemistry.mcmaster.ca/faculty/brennan.

[†] McMaster University.

[‡] York University.

(1) (a) Hage, D. S. *J. Chromatogr., B* **1998**, *715*, 3−38. (b) Hage, D. S. *Clin. Chem.* **1999**, *45*, 593−615. (c) Weller, M. G. *Fresenius J. Anal. Chem.* **2000**, *366*, 635−645. (d) Muronetz, V. I.; Sholukh, M.; Korpela, T. *J. Biochem. Biophys. Methods* **2001**, *49*, 29−47. (e) Baczek, T.; Kaliszan, R. *J. Biochem. Biophys. Methods* **2001**, *49*, 83−98. (f) Burgess, R. R.; Thompson, N. E. *Curr. Opin. Biotechnol.* **2002**, *13*, 304−308.

(2) (a) Hage, D. S.; Noctor, T. A. G.; Wainer, I. W. *J. Chromatogr., A* **1995**, *693*, 23−32. (b) Hofstetter, H.; Hofstetter, O. Schurig, V. *J. Microcolumn Sep.* **1998**, *10*, 287−291. (c) Hofstetter, O.; Lindstrom, H.; Hofstetter, H. *Anal. Chem.* **2002**, *74*, 2119−2125. (d) Fitos, I.; Visy, J.; Simonyi, M. *J. Biochem. Biophys. Methods* **2002**, *54*, 71−84.

(3) (a) Hsieh, Y. L.; Wang, H.; Elicone, C.; Mark, J.; Martin, S. A.; Regnier, F. *Anal. Chem.* **1996**, *68*, 455−462. (b) Wang, C.; Oleschuk, R.; Ouchen, F.; Li, J.; Thibault, P.; Harrison, D. *J. Rapid Commun. Mass Spectrom.* **2000**, *14*, 1377−1383. (c) Wang, S.; Regnier, F. E. *J. Chromatogr., A* **2001**, *913*, 429−436. (d) Peterson, D. S.; Rohr, T.; Svec, F.; Frechet, J. M. J. *J. Proteome Res.* **2002**, *1*, 563−568. (e) Peterson, D. S.; Rohr, T.; Svec, F.; Frechet, J. M. J. *Anal. Chem.* **2002**, *74*, 4081−4088. (f) Slysz, G. W.; Schriemer, D. C. *Rapid Commun. Mass Spectrom.* **2003**, *17*, 1044−1050.

(4) Prazeres, D.; Miguel F.; Cabral, J. M. S. In *Multiphase Bioreactor Design*; Cabral, J. M. S., Mota, M., Tramper, J., Eds.; Taylor & Francis Ltd.: London, U.K., 2001; pp 135−180.

(5) (a) Schriemer, D. C.; Bundle, D. R.; Li, L.; Hindsgaul, O. *Angew. Chem., Int. Ed. Engl.* **1998**, *37*, 3383. (b) Zhang, B.; Palcic, M. M.; Schriemer, D. C.; Alvarez-Manilla, G.; Pierce, M.; Hindsgaul, O. *Anal. Biochem.* **2001**, *299*, 173−182.

(6) (a) Baynham, M. T.; Patel, S.; Moaddel, R.; Wainer, I. W. *J. Chromatogr., B* **2002**, *772*, 155−161. (b) Moaddel, R.; Lu, L.; Baynham, M.; Wainer, I. W. *J. Chromatogr., B* **2002**, *768*, 41−53. (c) Moaddel, R.; Cloix, J.-F.; Ertem, G.; Wainer, I. W. *Pharm. Res.* **2002**, *19*, 104−107. (d) Moaddel, R.; Wainer, I. W. *J. Pharm. Biomed. Anal.* **2003**, *30*, 1715−1724.

(7) (a) Royer, C. A. *Prog. Biotechnol.* **2002**, *19*, 17−25. (b) Seemann, H.; Winter, R.; Royer, C. A. *J. Mol. Biol.* **2001**, *307*, 1091−1102.

10.1021/ac0352124 CCC: $27.50
Published on Web 04/10/2004

silica[8−12] or polymer[13] skeletons. These self-supporting columns do not require frits, have a bimodal pore structure that leads to high plate numbers, and have high through-pore volumes, which provides low back pressure and hence increased flow rates relative to bead columns. Together, these factors lead to shorter separation times and more efficient separations.[8−13] While the development of monolithic columns has been heralded as a breakthrough in reversed-phase chromatography, significant hurdles remain to be overcome to adapt this technology to the development of bioaffinity columns. A key issue with current monolithic columns is the harsh chemical processes that are used to form the columns (extreme pH values, organic solvents, high levels of urea) and, for silica columns, the fact that the column must be subjected to a high-temperature calcining step to remove entrapped organic polymers, which are added during processing to control porosity. Such conditions denature (or combust) entrapped proteins, making these processing methods incompatible with protein entrapment.

In recent years, it has been shown that a very mild and biocompatible sol−gel processing method can be used to entrap active proteins within a porous, inorganic silicate matrix.[14] In this method, a two-step processing method is used wherein a buffered solution containing the protein is added to the hydrolyzed silica sol to initiate gelation under conditions that are protein-compatible.[15] Numerous reports have appeared describing both fundamental aspects of entrapped proteins, such as their conformation,[16−18] dynamics,[19−21] accessibility,[18,22] reaction kinetics,[16,23] activity,[24] and stability,[25] and their many applications for catalysis and biosensing.[14,15] A number of reports also exist describing sol−gel-based immunoaffinity columns[26] and enzyme-based columns,[27] although in all cases these were formed by crushing protein-doped silica monoliths and then loading the bioglass into a column as a slurry.

Recent work on the development of protein-doped monolithic sol−gel columns has appeared from the groups headed by Zusman[28] and Toyo'oka.[29] Zusman's group has developed columns using glass fibers covered with antibody-doped sol−gel glass as a new support for affinity separation of tumor-associated antigens from blood. Toyo'oka's group has used capillary electrochromatography (CEC) both to prepare protein-doped sol−gel-based columns and to elute compounds. The columns were derived solely from TEOS or TMOS using a very high water/silicon and protein/silicon ratio, resulting in a column with sufficiently large pores to allow flow of eluent when charge is applied. While this is a significant advance, all chromatography was done using electroosmotic flow via CEC, which separates compounds on the basis of a combination of charge, mass, and affinity and is less compatible with MS detection due to the high ionic strength of the eluent. Also, these authors did not examine the interaction of

(8) Schulte, M.; Lubda, D.; Delp, A.; Dingenen, J. *J. High Resolut. Chromatogr.* **2000**, *23*, 100.
(9) Cabrera, K.; Lubda, D.; Eggenweiler, H.-M.; Nakanishi, H. M. *J. Hig Resolut. Chromatogr.* **2000**, *23*, 93.
(10) Nakanishi, K.; Shikata, H.; Ishizuka, N.; Koheiya, N.; Soga, N. *J. High Resolut. Chromatogr.* **2000**, *23*, 106.
(11) (a) Ishizuka, N.; Minakuchi, H.; Nakanishi, K.; Soga, N.; Tanaka, N. *J. Chromatogr., A* **1998**, *797*, 133. (b) Minakuchi, H.; Nakanishi, K.; Soga, N.; Ishizuka, N.; Tanaka, N. *J. Chromatogr., A* **1998**, *797*, 121. (c) Minakuchi, H.; Ishizuka, N.; Nakanishi, K.; Soga, N.; Tanaka, N. *J. Chromatogr., A* **1998**, *828*, 83. (d) Minakuchi, H.; Nakanishi, K.; Soga, N.; Ishizuka, N.; Tanaka, N. *Anal. Chem.* **1996**, *68*, 3498. (e) Ishizuka, N.; Minakuchi, H.; Nakanishi, K.; Hirao, K.; Tanaka, N. *Colloids Surf.* **2001**, *187−188*, 273. (f) Tanaka, N.; Kobayashi, H.; Nakanishi, K.; Minakuchi, H.; Ishizuka, N. *Anal. Chem.* **2001**, *73*, 420A. (g) Tanaka, N.; Nagayama, H.; Kobayashi, H.; Ikegami, T.; Hosoya, K.; Ishizuka, N.; Minakuchi, H.; Nakanishi, K.; Cabrera, K.; Lubda, D.; *J. High Resolut. Chromatogr.* **2000**, *23*, 111. (h) Motokawa, M.; Kobayashi, H.; Ishizuka, N.; Minakuchi, H.; Nakanishi, K.; Jinnai, H.; Hosoya, K.; Ikegami, T.; Tanaka, N. *J. Chromatogr., A* **2002**, *961*, 53−63.
(12) (a) Kato, M.; Sakai-Kato, K.; Toyo'oka, T.; Dulay, M. T.; Quirino, J. P.; Bennett, B. D.; Zare, R. N. *J. Chromatogr., A* **2002**, *961*, 45−51. (b) Dulay, M. T.; Quirino, J. P.; Bennett, B. D.; Zare, R. N. *J. Sep. Sci.* **2002**, *25*, 3−9. (c) Quirino, J. P.; Dulay, M. T.; Zare, R. N. *Anal. Chem.* **2001**, *73*, 5557−5563. (d) Dulay, M. T.; Quirino, J. P.; Bennett, B. D.; Kato, M.; Zare, R. N. *Anal. Chem.* **2001**, *73*, 3921−3926.
(13) (a) Xu, M.; Peterson, D. S.; Rohr, T.; Svec, F.; Frechet, J. M. J. *Anal. Chem.* **2003**, *75*, 1011−1021. (b) Hilder, E. F.; Svec, F.; Frechet, J. M. J. *Electrophoresis* **2002**, *23*, 3934−3953. (c) Xie, S.; Allington, R. W.; Frechet, J. M. J.; Svec, F. *Adv. Biochem. Eng./Biotechnol.* **2002**, *76*, 87−125.
(14) Gill, I. *Chem. Mater.* **2001**, *13*, 3404.
(15) Jin, W.; Brennan, J. D. *Anal. Chim. Acta* **2002**, *461*, 1.
(16) Zheng, L.; Reid, W. R.; Brennan, J. D. *Anal. Chem.* **1997**, *69*, 3940.
(17) Zheng, L.; Brennan, J. D. *Analyst* **1998**, *123*, 1735.
(18) Edmiston, P. L.; Wambolt, C. L.; Smith, M. K.; Saavedra, S. S. *J. Colloid Interface Sci.* **1994**, *163*, 395.
(19) Jordan, J. D.; Dunbar, R. A.; Bright, F. V. *Anal. Chem.* **1995**, *67*, 2436.
(20) Gottfried, D. S.; Kagan, A.; Hoffman, B. M.; Friedman, J. M. *J. Phys. Chem. B* **1999**, *103*, 2803.
(21) Doody, M. A.; Baker, G. A.; Pandey, S.; Bright, F. V. *Chem. Mater.* **2000**, *12*, 1142.
(22) Wambolt, C. L.; Saavedra, S. S. *J. Sol-Gel Sci. Technol.* **1996**, *7*, 53.
(23) Shen, C.; Kostic, N. M. *J. Am. Chem. Soc.* **1997**, *119*, 1304.
(24) (a) Braun, S.; Shtelzer, S.; Rappoport, S.; Avnir, D.; Ottolenghi, M. *J. Non-Cryst. Solids* **1992**, *147*, 739. (b) Avnir, D.; Braun, S.; Lev, O.; Ottolenghi, M. *Chem. Mater.* **1994**, *6*, 1605. (c) Wang, R.; Narang, U.; Prasad, P. N.; Bright, F. V. *Anal. Chem.* **1993**, *65*, 2671. (d) Ellerby, L. M.; Nishida, C. R.; Nishida, F.; Yamanaka, S. A.; Dunn, B.; Valentine, J. S.; Zink, J. I. *Science* **1992**, *225*, 1113. (e) Wu, S.; Ellerby, L. M.; Cohan, J. S.; Dunn, B.; El-Sayed, M. A.; Valentine, J. S.; Zink, J. I. *Chem. Mater.* **1993**, *5*, 115. (f) Dave, B. C.; Soyez, H.; Miller, J. M.; Dunn, B.; Valentine, J. S.; Zink, J. I. *Chem. Mater.* **1995**, *7*, 1431. (g) Yamanaka, S. A.; Nishida, F.; Ellerby, L. M.; Nishida, C. R.; Dunn, B.; Valentine, J. S.; Zink, J. I. *Chem. Mater.* **1992**, *4*, 495. (h) Dave, B. C.; Dunn, B.; Valentine, J. S.; Zink, J. I. *Anal. Chem.* **1994**, *66*, 1120A. (i) Blyth, D. J.; Aylott, J. W.; Richardson, D. J.; Russell, D. A. *Analyst* **1995**, *120*, 2725. (j) Aylott, J. W.; Richardson, D. J.; Russell, D. A. *Analyst* **1997**, *122*, 77. (k) Williams, A. K.; Hupp, J. T. *J. Am. Chem. Soc.* **1998**, *120*, 4366.
(25) (a) Braun, S.; Rappoport, S.; Zusman, R.; Avnir, D.; Ottolenghi, M. *Mater. Lett.* **1990**, *10*, 1. (b) Heichal-Segal, O.; Rappoport, S.; Braun, S.; *Biotechnology* **1995**, *13*, 798. (c) Reetz, M. T.; Zonta, A.; Simpelkamp, J.; *Biotechnol. Bioeng.* **1996**, *49*, 527. (d) Narang, U.; Prasad, P. N.; Bright, F. V.; Kumar, K.; Kumar, N. D.; Malhotra, B. D.; Kamalasanan, M. N.; Chandra, S. *Chem. Mater.* **1994**, *6*, 1596. (e) Narang, U.; Prasad, P. N.; Bright, F. V.; Ramanathan, K.; Kumar, N. D.; Malhotra, B. D.; Kamalasanan M. N.; Chandra, S. *Anal. Chem.* **1994**, *66*, 3139. (f) Jordan, J. D.; Dunbar, R. A.; Bright, F. V. *Anal. Chim. Acta* **1996**, *332*, 83. (g) Yamanaka, S. A.; Dunn, B.; Valentine, J. S.; Zink, J. I. *J. Am. Chem. Soc.* **1995**, *117*, 9095. (h) Kauffmann, C.; Mandelbaum, R. T. *J. Biotechnol.* **1998**, *62*, 169.
(26) (a) Bronshtein, A.; Aharonson, N.; Avnir, D.; Turniansky, A.; Altstein, M. *Chem. Mater.* **1997**, *9*, 2632. (b) Altstein, M.; Bronshtein, A.; Glattstein, B.; Zeichner, A.; Tamiri, T.; Almong, J. *Anal. Chem.* **2001**, *73*, 2461. (c) Bronshtein, A.; Aharonson, N.; Turniansky, A.; Altstein, M. *Chem. Mater.* **2000**, *12*, 2050. (d) Cichna, M.; Knopp, D.; Niessner, R. *Anal. Chim. Acta* **1997**, *339*, 241. (e) Cichna, M.; Markl, P.; Knopp, D.; Niessner, R. *Chem. Mater.* **1997**, *9*, 2640. (f) Schedl, M.; Wilharm, G.; Achatz, S.; Kettrup, A.; Niessner, R.; Knopp, D. *Anal. Chem.* **2001**, *73*, 5669−5676. (g) Spitzer, B.; Cichna, M.; Markl, P.; Sontag, G.; Knopp, D.; Niessner, R. *J. Chromatogr., A* **2000**, *880*, 113.
(27) Cichna, M. *J. Sol-Gel Sci. Technol.* **2003**, *26*, 1159−1164.
(28) Zusman R.; Zusman, I. *J. Biochem. Biophys. Methods* **2001**, *49*, 175−187.
(29) (a) Sakai-Kato, K.; Kato, M.; Toyo'oka, T. *Anal. Chem.* **2002**, *74*, 2943−2949. (b) Kato, M.; Sakai-Kato, K.; Matsumoto, N.; Toyo'oka, T. *Anal. Chem.* **2002**, *74*, 1915−1921. (c) Sakai-Kato, K.; Kato, M.; Toyo'oka, T. *Anal. Biochem.* **2002**, *308*, 278−284. (d) Sakai-Kato, K.; Kato, M.; Nakakuki, H.; Toyo'oka, T. *J. Pharm. Biomed. Anal.* **2003**, *31*, 299−309. (e) Sakai-Kato, K.; Kato, M.; Toyo'oka, T. *Anal. Chem.* **2003**, *75*, 388−393. (f) Kato, M.; Matsumoto, N.; Sakai-Kato, K.; Toyo'oka, T. *J. Pharm. Biomed. Anal.* **2003**, *30*, 1845−1850.

potential inhibitors with entrapped proteins on-column. This is a particularly important issue given the emergence of high-throughput screening (HTS) methods based on immobilized enzymes.[5,6,30]

In this paper, we describe the development of biocompatible, bimodal meso/macroporous silica materials that can be used for protein entrapment and show that capillary columns based on these materials can be prepared that are suitable for pressure-driven liquid chromatography and compatible with electrospray mass spectrometry (ESI-MS) detection. Our columns are prepared using a mixture of the protein-compatible silica precursor diglycerylsilane (DGS),[31] poly(ethylene oxide) (PEO, MW 10 000), which controls morphology, (aminopropyl)triethoxysilane (APTES), which provides cationic sites that counterbalance the anionic charge of the silica to reduce nonselective interactions,[28] and a buffered solution of the protein of interest to provide bioaffinity sites within the column. The resulting sol mixture is loaded into fused-silica capillaries (150−250-μm i.d.), whereupon spinodal decomposition of the PEO-containing sol occurs, followed by gelation of the silica.[8−11] The phase separation of the polymer from the silica results in a bimodal pore distribution, which produces large macropores (> 0.1 μm) to allow good flow of eluent with minimal back pressure, and mesopores (~3−5-nm diameter) that retain a significant fraction of the entrapped protein.

As a specific application of the new bioaffinity columns, we examined the ability of small enzyme inhibitors to interact with an entrapped enzyme and thus be retained on the column. The enzyme chosen for this study was the clinically relevant protein dihydrofolate reductase (DHFR). DHFR catalyzes the reduced nicotinamide adenine dinucleotide phosphate (NADPH)-dependent reduction of dihydrofolate (DHF) to tetrahydrofolate, which is then used as a cofactor in the biosynthesis of thymidylate, purines, and several amino acids.[32−34] DHFR is an essential enzyme in the cell and is the target for antifolate drugs.[35] An advantage of this protein is that there are a large number of known DHFR inhibitors that span 5 decades of affinity (~1 nM to 10 μM), providing a useful model system for examining the binding of inhibitors to the entrapped enzyme.[35] This enzyme has also been shown to remain active and accessible when entrapped in DGS-derived materials.[31]

Examination of ligand binding was done via frontal affinity chromatography with mass spectrometric detection (FAC/MS). This method has recently been promoted as a potential screening tool that is amenable to compound mixtures.[5] The basic premise is that continuous infusion of a compound will allow for equilibration of the ligand between the free and bound states, where the precise concentration of free ligand is known. In this case, the breakthrough time of the compound will correspond to the affinity of the ligand for the immobilized biomolecule—ligands with higher affinity will break through later. As shown herein, DHFR-loaded columns derived by the sol−gel method are suitable for FAC/MS-based screening of ligand mixtures and can be used to identify nanomolar inhibitors of the immobilized protein.

EXPERIMENTAL SECTION

Chemicals. Tetraethyl orthosilicate (TEOS, 99.999%), dimethyldimethoxysilane (DMDMS, 98%), and APTES were obtained from Aldrich (Oakville, ON, Canada). Diglycerylsilane precursors were prepared from TEOS as described below. Human serum albumin (HSA), trimethoprim, pyrimethamine, DHF, NADPH, folic acid, dithiothreitol (DTT) poly(ethylene glycol) (PEG/PEO, MW 2000−100 000) poly(allylamine) (MW 17 000 kDa), and fluorescein were obtained from Sigma (Oakville, ON, Canada). Coumarin and 5-(and −6) carboxyfluorescein, succinimidyl ester were obtained from Molecular Probes Inc. (Eugene, OR). Recombinant dihydrofolate reductase (from *Escherichia coli*), which was affinity purified on a methotrexate column, was provided by Professor Eric Brown (McMaster University).[36] Fused-silica capillary tubing (150−250-μm i.d., 360-μm o.d., polyimide coated) was obtained from Polymicro Technologies (Phoenix, AZ). All water was distilled and deionized using a Milli-Q synthesis A10 water purification system. All other reagents were of analytical grade and were used as received.

Procedures. *Preparation of DGS.* TEOS was distilled to remove any residual water, and a neat mixture of the anhydrous TEOS (2.08 g, 10.0 mmol) and anhydrous glycerol (1.84 g, 20.0 mmol) was heated at 130 °C for 36 h, during which time EtOH was distilled off. Complete removal of EtOH and unreacted starting materials at 140 °C in vacuo gave DGS as a solid compound that was not contaminated with residual ethanol. Structural characterization of DGS by NMR and the properties of DGS-derived silica will be reported elsewhere.[37]

Preparation of Columns. Prior to loading columns, the inner surface of the fused-silica capillary was coated with APTES to promote electrostatic binding of the monolithic silica column. The capillary was first washed with 3−4 volumes of 1 M NaOH, H_2O, 1 M HCl, H_2O, and EtOH. At this point, 1 mL of 2% (v/v) APTES in absolute EtOH was loaded into the column and left to react for 12 h at 110 °C, after which the excess APTES was washed out with water and the capillary was dried for 12 h at 110 °C.

Silica sols were prepared by first mixing 1 g of DGS (finely ground solid) with 990 μL of H_2O and, optionally, 10 μL of 1 M HCl to yield ~1.5 mL of hydrolyzed DGS, after 15−25 min of sonication. The hydrolyzed DGS was filtered through a 0.45-μm syringe to remove particulates before use. A second aqueous solution of 50 mM HEPES at pH 7.5 was prepared containing 16% (w/v) PEO (MW = 10 000) and 0.6% (v/v) APTES. This aqueous solution also contained ~20 μM DHFR. A 100-μL aliquot of the buffer/PEG/APTES/DHFR solution was mixed with 100 μL of hydrolyzed DGS, and the mixture was immediately loaded via syringe pump into a fused-silica capillary (~2 m long, 150−250-μm i.d.). The final composition was of the solution was 8% w/v PEO (10 000), 0.3% v/v APTES, and 10 μM DHFR in 25 mM HEPES buffer. The mixture became cloudy due to spinodal decomposition (phase separation) over a period of 1−3 s about 2−3 min before silica polymerization (~10 min) to generate a

(30) Macbeath, G.; Schreiber, S. L. *Science* **2000**, *289*, 1760.
(31) Besanger, T. R.; Chen, Y.; Deisingh, A. K.; Hodgson, R.; Jin, W.; Mayer, S.; Brook, M. A.; Brennan, J. D. *Anal. Chem.* **2003**, *75*, 2382−2391.
(32) Hitchings, G. H. *Angew. Chem., Int. Ed. Engl.* **1989**, *29*, 879.
(33) Stone, S. R.; Morrison, J. F. *Biochemistry* **1988**, *27*, 5493.
(34) Benkovic, S. J.; Fierke, C. A.; Naylor, A. M. *Science* **1988**, *239*, 1105.
(35) Polshakov, V. I.; Biekofsky, R. R.; Birdsall, B.; Feeney, J. *J. Mol. Struct.* **2002**, *602−603*, 257.
(36) Zolli-Juran, M.; Cechetto, J. D.; Harlen, H.; Daigle, D. M.; Brown, E. D. *Bioorg. Med. Chem. Lett.* **2003**, *13*, 2493.
(37) Brook, M. A.; Chen, Y.; Guo, K.; Zhang, Z.; Jin, W.; Deisingh, A.; Cruz-Aguado, J.; Brennan, J. D. *J. Sol-Gel Sci. Technol.*, in press.

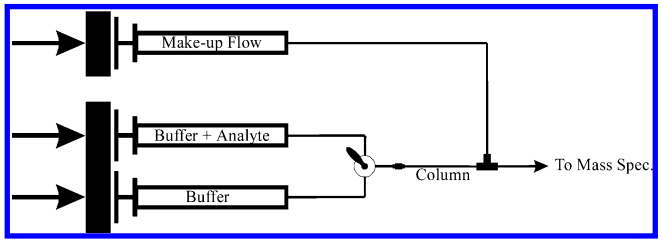

Figure 1. Schematic of the apparatus used for FAC/MS. A switch valve is used to switch from buffer to buffer + analyte, allowing continuous infusion of analytes onto the column. The column outlet is connected to a mixing tee for addition of makeup buffer that flows directly into the PE/Sciex API 3000 triple-quadrupole mass spectrometer.

hydrated macroporous monolithic column containing entrapped protein. Phase separation was easily visualized by eye, while gelation time was determined by measuring the loss of flow of the material. After loading of the sol−gel mixture, the monolithic columns were aged for a minimum of 5 days at 4 °C and then cut into 10-cm lengths before use. In some cases, a final concentration of either 0.03% polyallylamine (PAM, MW 17 000) or 0.3% DMDMS was added to the columns instead of APTES to examine the effects of surface derivatization on nonselective retention.

Characterization of Silica Morphology. The morphology of the column was assessed using nitrogen adsorption porosimetry (for characterization of mesopores) or mercury intrusion porosimetry and scanning electron microscopy (SEM) for characterization of macropores. Nitrogen porosimetry of completely dried monoliths was performed on a Quantachrome Autosorb-1 surface area/pore size analyzer. Before analysis, the monoliths were washed copiously to remove any entrapped glycerol, crushed to a fine powder, freeze-dried, and outgassed at 120 °C for 4 h to remove air and bound water from the surface of the powder. The pressure was measured as nitrogen was adsorbed and desorbed at a constant temperature of −196 °C. Using the desorption branch of the resulting isotherm, the average pore size and distribution of pore sizes was determined using the Barrett, Joyner, and Halenda calculation.[38] Samples were prepared in an identical manner for Hg intrusion porosimetry and were measured using a Quantachrome PoreMaster 60 instrument. The contact angle used was 140°. Both high- and low-pressure data were obtained on the same sample, covering the pressure range from 0.8 to 59 658 psia (265.5 μm to 3.58 nm pore diameter range). SEM analysis was done by cutting the capillary to expose a fresh surface, which was then coated with a gold film under vacuum to improve conductivity. Imaging was performed at 10 kV using a JEOL 840 scanning electron microscope.

FAC/MS Studies. The frontal affinity chromatography/mass spectrometer system is shown in Figure 1. Syringe pumps (Harvard Instruments model 22) were used to deliver solutions, and a flow-switching valve was used to toggle between the assay buffer and the solution containing the compound mixture. This solution was then pumped through the column to achieve equilibrium. Effluent was combined with suitable organic modifiers to assist in the generation of a stable electrospray and detectability of the sprayed components using a triple-quadrupole MS system (PE/Sciex API 3000). This configuration allows for maximum flexibility in compound introduction. Full operation of FAC/MS methods requires frequent flow switching between two solutions connected to the head of the column. An Upchurch microinjection valve allows syringe contents to be exchanged during operation. Columns were interfaced to the FAC system using Luer capillary adapters (Luer adapter, ferrule and green microtight sleeve from Upchurch (P-659, M-100, F-185X)). All other connections between components were achieved using fused-silica tubing.

Typical FAC/MS experiments involved infusion of mixtures of compounds containing 1−200 nM concentrations of each compound, including coumarin and fluorescein as void markers, folic acid (micromolar substrate), and pyrimethamine and trimethoprim (nM inhibitors). Before the first run, the column was flushed with 0.05 M NH_4OAc buffer (pH 6.6, 100 mM NaCl) for 30 min at different flow rates (from 1 to 5 $\mu L \cdot min^{-1}$) to remove any glycerol and nonentrapped protein and then equilibrated with 2 mM NH_4OAc for 30 min at different flow rates (from 1 to 5 $\mu L \cdot min^{-1}$). All compounds tested were present in 2 mM NH_4OAc and were delivered at a rate of 5 $\mu L \cdot min^{-1}$ using the syringe pump. The makeup flow (used to assist in the generation of a stable electrospray) consisted of methanol containing 10% (v/v) NH_4-OAc buffer (2 mM) and was delivered at 5 $\mu L \cdot min^{-1}$, resulting in a total flow rate of 10 $\mu L \cdot min^{-1}$ entering the mass spectrometer. The mass spectrometer was operated in multiple reaction monitoring mode with simultaneous detection of m/z 147 → 103 (coumarin); 249 → 177 (pyrimethamine); 291 → 230 (trimethoprim); 333 → 287 (fluorescein), and 442 → 295 (folic acid).

Characterization of Column Performance. Columns of 10-cm length were prepared containing no protein (blanks), initial loadings of 50 pmol of active DHFR, or 50 pmol of DHFR that was partially denatured by boiling prior to use or 50 pmol of HSA (selectivity control). In all cases, FAC/MS measurements were performed using the five-compound mixture described above and the resulting frontal chromatograms were used to evaluate nonselective interactions of compounds with the column, the reversibility of binding, the potential for regeneration of columns, and the level of leaching of entrapped protein.

Columns that contained active DHFR were further characterized by monitoring the breakthrough volume (obtained by multiplying flow rate by breakthrough time) as a function of analyte concentration using either pyrimethamine or trimethoprim. In each case, the data were fit to the following equation:[5a]

$$V = V_0 + \frac{B_t}{[A] + K_d} \quad (1)$$

where V_0 is the void volume (μL), V is the retention volume (μL), [A] is the analyte concentration (μM), K_d is the binding constant of the ligand to the protein (μM) and B_t is the total picomoles of active protein in the column, based on one active site per enzyme molecule.

Characterization of Protein Leaching. DHFR was fluorescently labeled using 5-(and −6)-carboxyfluorescein, succinimidyl ester. A reaction mixture containing 0.58 mM DHFR, 1.9 mM 5-(and −6)-carboxyfluorescein, succinimidyl ester, and 150 mM sodium bicarbonate was incubated at room temperature for 2 h. The mixture was then exhaustively dialyzed at 4 °C against 25 mM

(38) Barrett, E. P.; Joyner, L. G. Halenda, P. H. *J. Am. Chem. Soc.* **1951**, *73*, 373.

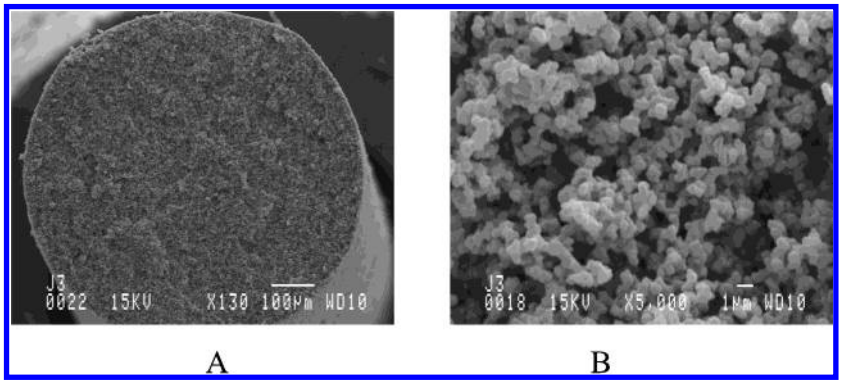

Figure 2. SEM images of a sol−gel-derived column containing DGS/PEO/APTES after 5 days of aging. Panel A: image of monoliths formed in 1-mm capillaries that pulled away from the capillary wall and were removed from the capillary under flow; Panel B: magnified image of a monolith in a 250-μm capillary showing the bimodal pore distribution within the sol−gel-derived monolith.

HEPES (pH 7.5, 5 × 1000-fold excess over a 40-h period) to remove unbound fluorescein. Columns containing fluorescently labeled DHFR were prepared as described above. The running buffer used for FAC/MS was passed through the column at a flow rate of 5 μL·min^{-1}, and fractions were collected over a period of 1 h for 8 h. The fluorescence emission intensity of each fraction was compared to a standard curve of emission intensity versus concentration of fluorescently labeled DHFR stock to determine the concentration of DHFR present in the eluted buffer. After the 8-h elution experiment, the monolith was dissolved by infusing 25 μL of 1 M NaOH. The column contents were then neutralized with 1 M Tris-HCl, pH 8.3, and the emission intensity was compared to a calibration curve to determine the concentration of DHFR remaining in the column. All fluorescence measurements were made using a Tecan Saphire microplate reader operated in top-read mode using an excitation wavelength of 488 nm and an emission wavelength of 515 nm with 5-nm band-passes in both the excitation and emission paths.

DHFR Stability in 2 mM Ammonium Acetate. DHFR was diluted to 40 nM in 2 mM ammonium acetate, (which therefore contained 3 μM HEPES and 2 μM NaCl) and was incubated for 8 h. At 1-h intervals, 100-μL aliquots were mixed with 100 μL of a solution containing 50 mM Tris-HCl pH 7.5, 2 mM DTT, 100 μM NADPH, and 100 μM DHF. DHFR activity was measured by monitoring the decrease in absorbance at 340 nm using a Tecan Saphire microplate reader. Activity data are reported relative to the activity obtained from a DHFR sample that was diluted in 50 mM Tris-HCl, pH 7.5, containing 2 mM DTT.

RESULTS

Column Formation and Optimization. It was critical that the bioaffinity columns be fabricated using protein-compatible processes; thus, several issues were addressed to produce a viable monolithic bioaffinity column. Key goals to achieve when developing monolithic bioaffinity columns were as follows: (1) to produce a biocompatible column matrix that entrapped biomolecules in an active form; (2) to have spinodal composition occur after column loading but before gelation of the silica phase to promote macroporosity; (3) to avoid shrinkage and cracking of the column, which would introduce unwanted flow channels; (4) to minimize protein leaching after gelation of the silica; and (5) to minimize nonselective interactions between small molecules and the silica matrix. A variety of parameters were optimized to achieve this goal, including the silica precursor (TEOS vs DGS), silica concentration (1−10 mol %), gelation pH (5−8), ionic strength (0−100 mM), and PEO concentration (2−12% w/v) and molecular weight (2000−100 000). While several compositions produced viable columns, the best performance was obtained using a composition derived from the protein-compatible precursor DGS, which contained an initial level of 3.3 mol % SiO_2. Lower levels led to columns that would slowly dissolve in the mobile phase, while higher levels gelled too quickly to allow facile column loading. Optimal gelation conditions were achieved under mild conditions at 4 °C, pH ∼7 with an ionic strength of 25 mM. Macroporosity could be obtained using a variety of PEO concentrations and molecular weights (see below); however, we selected columns that contained 8% w/v of MW 10 000 PEO. Phase separation occurred for molecular weight values of 10 000 or higher and at levels of 2% w/v or higher for 10 000 or higher molecular weight PEO. An optimal level of 8% w/v for MW 10 000 PEO was selected owing to the good homogeneity and reproducibility obtained for forming columns using this composition and because higher levels or molecular weights of PEO produced solutions that were too viscous to allow facile loading of the column.

Early versions of columns used untreated, NaOH, methacryloxypropyltrimethoxysilane or 3-glycidoxypropyltrimethoxysilane-treated capillaries as supports. However, it was often observed that the monolith could be pushed out of the capillary at higher flow rates. To overcome this problem, the inner surface of the capillary was pretreated with APTES, which provided electrostatic bonding between the anionic silica monolith and the cationically modified capillary surface. In such columns, flow rates as high as 500 μL·min^{-1} could be achieved with no occurrences of monolith detachment from the capillary.

Column Characterization. Figure 2 shows scanning electron microscopy images of the DGS/PEO/APTES monolithic silica stationary phase. Panel A shows an image of a 1.0-mm-diameter column that had been extruded from an uncoated capillary and shows that the silica forms a self-supporting monolith. Panel B shows a high-magnification image of a monolith within a 250-μm capillary, showing the macroporous nature of the silica skeleton. The silica matrix appears to be composed primarily of silica beads that are 1−2 μm in diameter and are linked together to form a continuous monolith. The voids (through-pore spaces) are on the

Table 1. Mercury Intrusion Porosimetry Data for Macroporous Silica Samples Used for Column Development. All Samples Contain 8 wt % of Polymer

sample	total pore vol (cm^3)	through-pore vol (cm^3)	bulk (particle) density (g/cm^3)	interparticle porosity (%)		av macropore diam (μm)
				through-pores	mesopores	
DGS + PEO MW 2000	2.28	0.15	0.35	5.0	75.0	1.22
DGS + PEO MW 10 000	1.74	0.55	0.43	23.5	51.2	0.49
DGS + PEO MW 100 000	2.25	0.62	0.36	20.5	59.9	2.91

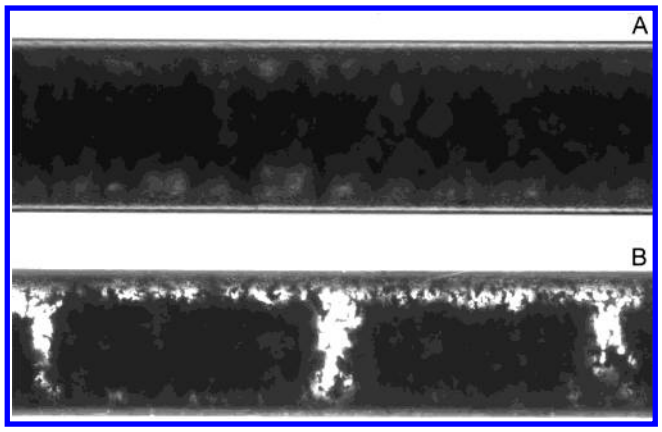

Figure 3. Bright-field images of a filled capillary (250-μm i.d.) after 3 months of aging in buffer (panel A) and after 24 h of storage in a desiccator (panel B).

order of 1 μm in diameter (see mercury intrusion porosimetry data below) and provide sufficient void volume to allow good flow of liquids with low back pressure. Overall, the macroporous morphology of the columns appears to be quite similar to that reported by Tanaka for reversed-phase columns (skeleton size of 1−2 μm, through-pore diameter of 2−8 μm[11h]), although it is important to note that in the case of Tanaka's columns the PEO was removed by pyrolysis before imaging.

Attempts to image monoliths within 150−250-μm-i.d. capillary columns via SEM showed that the introduction of the columns to ultrahigh vacuum (UHV) produced pullaway of the monolith from the capillary wall. To avoid UHV, the monoliths were imaged using bright-field microscopy. Figure 3 shows a bright-field image of a filled capillary (250-μm i.d.) after 3 months of aging in buffer (panel A) and clearly shows that the monolith completely fills the capillary with no pullaway. The lighter areas at the edges of the capillary in this image are due to differences in light diffraction. This was confirmed by testing the flow through 3-month-old columns, which was identical to that obtained from fresh columns (data not shown). Panel B shows the same monolith after 24 h of storage in a desiccator. Upon removal of entrapped water, the silica monolith shrinks significantly and exhibits cracking and pullaway. These results show that columns must be stored in a wet state to maintain column integrity. Such storage conditions are also necessary to maintain the activity of entrapped proteins.

Mercury intrusion porosimetry was done on PEO-doped samples to better assess the nature of the macropores in the various materials. Table 1 shows the data obtained for samples containing 8 wt % of MW 2000, 10 000, and 100 000 PEO. While all materials contained macropores, the size and proportion of macropores was highly dependent on the molecular weight of the PEO used. For MW 2000 PEO-doped samples, only 5% of the pore volume was occupied by macropores with an average diameter of 1.2 μm. Columns formed from such materials did not show good flow properties and thus were not examined further. Samples containing MW 10 000 PEO (which were used for subsequent FAC/MS studies described below) had a much higher proportion of macropores (23%) with an average pore diameter of ~0.5 μm. Increasing the molecular weight of PEO to 100 000 led to a similar proportion of macropores (20%), but in this case, the average macropore diameter was much higher than was observed with MW 10 000 PEO (almost 3 μm). While such materials led to columns that showed good flow properties, the material underwent phase separation and gelation rapidly, which made it difficult to reproducibly fill the columns.

BET measurements were performed on PEO-doped samples to assess the morphology of the mesopores within the silica skeleton (note: measurements were done only for samples that were not pyrolyzed). Table 2 shows the mean pore diameter, surface area, and volume occupied by mesopores within the column. Although the drying process decreases pore diameters by a factor of ~10-fold,[39] the differences in the pore sizes of the dried samples are likely to reflect the relative pore size differences in the wet, chromatographic matrix. While PEO is primarily responsible for the formation of macropores in our materials, it is evident that the addition of MW 10 000 PEO, dramatically alters the fraction of mesopores (2−50-nm diameter) relative to micropores (<2 nm) in favor of mesopores, although it leads to only minor decreases in surface area relative to pure DGS. The addition of PEO also produces a higher total pore volume and a slightly larger average mesopore diameter, both of which should result in somewhat better flow properties. When considered together with the SEM and Hg intrusion porosimetry data, it is apparent that the columns have the desired meso/macroporous morphology, although at this point we have not yet optimized the through-pore size and skeleton size of the monolithic silica columns.

Bioaffinity Column Performance. A key consideration in the development of bioaffinity columns for FAC/MS applications is to minimize nonselective adsorption of analytes to the column matrix while maximizing the retention of compounds owing to selective binding to the entrapped protein. Figure 4 shows frontal chromatograms of unmodified columns relative to columns containing dimethyldimethoxysilane-, aminopropylsilane-, or poly-

(39) Bhatia, R. B.; Brinker, C. J.; Gupta, A. K.; Singh, A. K. *Chem. Mater.* **2000**, *12*, 2434.

Table 2. BET Data for Several Silica Compositions

	expt no.		
	D-4	D-11	D-10
precursor	DGS	DGS + PEO MW 2000	DGS + PEO MW 10 000
surface area data (m^2/g)			
single-point BET area	581	565	560
multipoint BET area	596	575	574
Langmuir surface area	1668	1653	1915
micropore area	473	418	268
meso pore area	124	157	305
cumulative adsorption surface area	593	503	548
cumulative desorption surface area	586	520	648
pore volume data (cm^3/g)			
total pore volume	0.467 (<56.2 nm)	0.476 (<51.2 nm)	0.506 (<54.2 nm)
cumulative adsorption pore vol ($r = 30-1$ nm)	0.422	0.399	0.459
cumulative desorption pore vol ($r = 30-1$ nm)	0.430	0.414	0.506
micropore vol	0.342	0.306	0.210
pore size data (nm)			
average pore radius	1.56	1.65	1.76

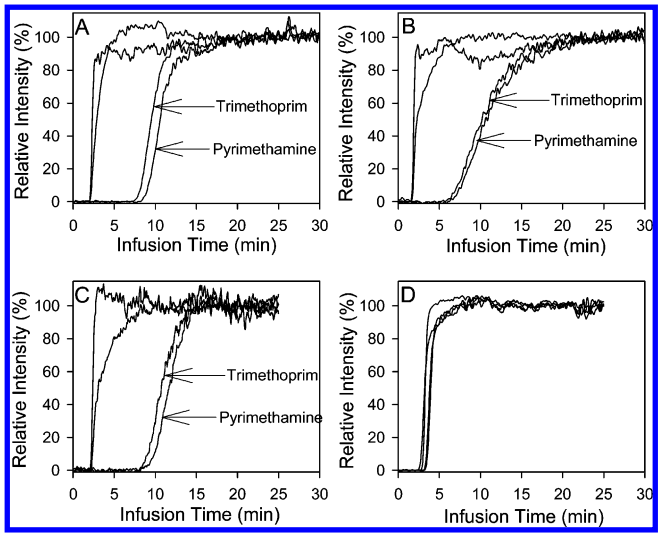

Figure 4. FAC/MS data showing the effects of surface modification on nonselective adsorption. Panel A: unmodified DGS/PEO monoliths. Panel B: DGS/PEO monoliths containing 0.3% w/v DMDMS. Panel C: DGS/PEO monoliths containing 0.03% w/v poly(allylamine) MW 17 000. Panel D: DGS/PEO monoliths containing 0.3% w/v APTES. The order of elution for all chromatographs is methotrexate, fluorescein, trimethoprim, and pyrimethamine.

(allylamine)-derivatized silica. These additives allowed us to examine charged and uncharged additives and to modify the hydrophobicity of the column so as to modulate interactions of analytes with the silica. As shown in panel A, the unmodified silica has a tendency to retain cationic species (pyrimethamine and trimethoprim) but does not retain either anionic or neutral species. Addition of either DMDMS or PAM did not significantly alter the retention properties, possibly owing to the low levels at which these could be employed before reducing column performance. However, even low levels of APTES led to almost complete removal of interactions between the silica matrix and cationic analytes, while retaining the low degree of nonselective adsorption of anionic and neutral species, in agreement with previous observations by Zusman for sol−gel-based glass fiber affinity columns.[28] Higher levels of APTES caused retention of anionic species, and thus, 0.3% APTES was found to be optimal for minimizing nonselective retention. Recent studies using time-resolved fluorescence anisotropy to probe adsorption of the charged fluorescent probes onto APTES-modified silica surfaces confirms that 0.3% (v/v) APTES effectively creates a zwitterionic surface with no net attraction or repulsion of charged species.[40] This level of APTES is also the maximum amount that can be used before flocculation of sols will occur. Importantly, this surface maintained its ability to block nonselective retention over a period of months, indicating that the APTES formed a stable surface coating that did not change in composition with time.

Figure 5 shows FAC/MS traces obtained for elution of mixtures of DHFR inhibitors and control compounds through DGS/PEO/APTES columns containing no protein, active DHFR, partially denatured DHFR, or HSA, a protein that does not bind DHFR inhibitors. The blank column shows the expected breakthrough of all compounds in the first few minutes, indicative of minimal nonselective interactions, showing that normal-phase silica chromatography had been suppressed. Panel B shows significant retention of the two DHFR inhibitors, trimethoprim ($K_d = 4$ nM, elution time of 39 min) and pyrimethamine ($K_d = 45$ nM, retention time 55 min), less retention of a weakly binding substrate (folic acid, $K_d = 11$ μM, retention time 7 min), and no retention of nonselective ligands (fluorescein, coumarin; retention time 2 min). This result indicates that DHFR is active when entrapped in the column, in agreement with recent results from our group showing good activity of DHFR when entrapped in DGS derived materials.[31] Upon boiling DHFR prior to entrapment, all DHFR-binding ligands show significantly reduced retention times, consistent with partial denaturation of the protein. It should be noted that DHFR is known to be remarkably stable to thermal denaturation and that thermal unfolding of DHRF is partially reversible.[41] Thus, it is not surprising that partial binding affinity

(40) Tleugabulova, D.; Zhang, Z.; Chen, Y.; Brook, M. A.; Brennan, J. D. *Langmuir* **2004**, *20*, 848−854.
(41) Iwakura, M.; Honda, S. *J. Biochem.* **1996**, *119*, 414−420.

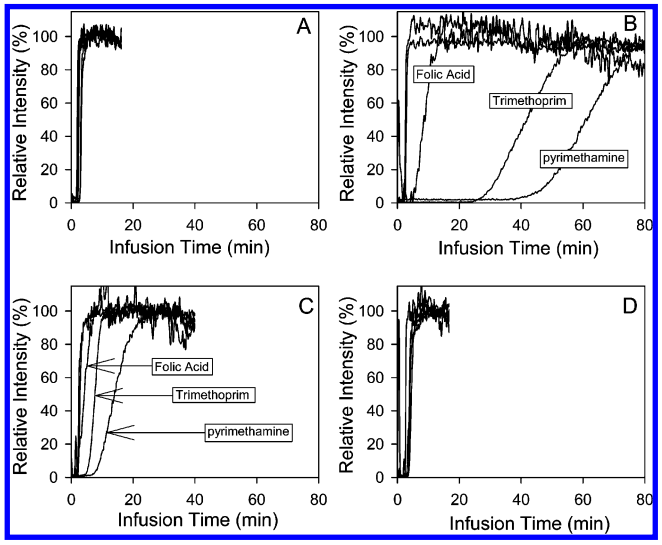

Figure 5. Typical FAC/MS traces obtained using protein-loaded and blank DGS/PEO/APTES monolithic columns. Panel A: blank columns containing no protein. Panel B: column containing 50 pmol of DHFR (initial loading). Panel C: column containing an initial loading of 50 pmol of heat-denatured DHFR. Panel D: columns containing an initial loading of 50 pmol of HSA. Coumarin, pyrimethamine, trimethoprim, and folic acid were infused at 20 nM. Fluorescein was infused at 100 nM. All traces are normalized to the maximum signal obtained after compound breakthrough.

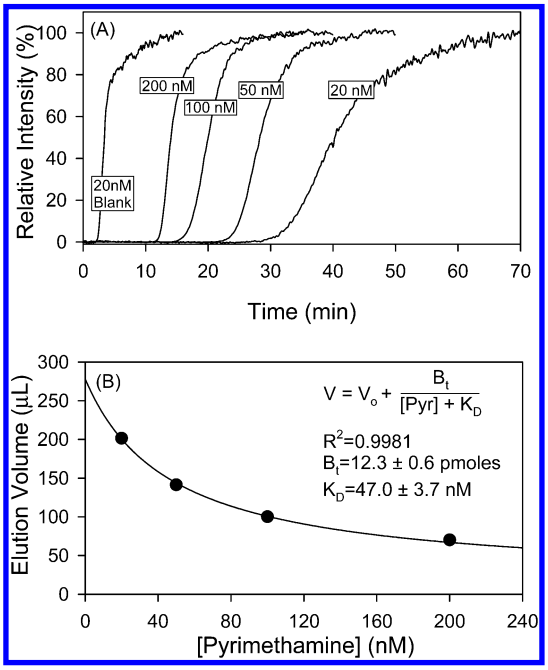

Figure 6. Determination of K_d and B_t values for DHFR columns based on the effect of ligand concentration on breakthrough volume. Panel A: superimposed FAC/MS traces at four different ligand concentrations relative to a blank column; Panel B: plot of V vs [A]. Note that the data were obtained from the first run performed on four individual DHFR loaded columns and one blank column.

is retained even after heat denaturation. As a secondary control, a column containing entrapped HSA was examined. As shown in panel D there is essentially no binding beyond that obtained in a blank column. Thus, retention of the ligands is a consequence of selective interactions between the ligands and DHFR. The reversal in the expected elution times for trimethoprim and pyrimethamine (based on their respective K_d values) is not fully understood at this time but may be related to differences in on and off rates, which are likely to play a significant role in determining the overall retention time of compounds on the column. This is being examined in further detail and will be discussed in a future report.

To further explore the properties of the DHFR-doped columns, the effect of ligand concentration on elution time was examined for both pyrimethamine and trimethoprim. As the concentration of ligand increases, one expects the column to saturate more rapidly for a given flow rate, and thus, the compound is expected to break through earlier. By plotting elution volume against analyte concentration, one can determine the amount of protein immobilized (B_t) and the dissociation constant of the protein directly on the column. Figure 6 shows breakthrough curves for pyrimethamine at various concentrations, and the resulting plot of V vs [A]. From these data one extracts a total protein concentration of 12 pmol on the column and a K_d of 47 nM. The K_d value is essentially identical to that in solution (37 nM) and is in excellent agreement with the value obtained for DHFR entrapped in DGS-derived materials (46 nM).[31] The data obtained from trimethoprim provided a K_d value of 21 nM and a B_t value of 7 pmol (data not shown). The K_d value for trimethoprim in DGS is 3 nM; thus, the affinity of the inhibitor is somewhat lower than previously reported but is still in the nanomolar range and therefore would be considered a "hit" in a high-throughput screen. The higher K_d value for trimethoprim obtained by FAC/MS may be the result of the low ionic strength buffer used in these experiments. The B_t values indicate that only 15−25% of the initially loaded protein remained active and accessible. The remainder (75−85%) of the initial protein present was therefore either denatured, inaccessible, or removed from the column during column conditioning. To distinguish between these possibilities, two experiments were performed. To test protein leaching, we fluorescently labeled DHFR and entrapped it in the column. We then washed the column with 2 mM ammonium acetate buffer for 8 h and determined the amount of protein remaining in the column each hour and at the end of the 8-h wash. As shown in Figure 7A, a large fraction of protein leached in the first hour (corresponding to the time used to condition the column), after which leaching of protein occurred slowly. After 8 h, there was still ∼30% of the initial protein entrapped in the column and leaching was minimal. In a second experiment, we flushed the column for 8 h with 2 mM ammonium acetate (the running buffer) before the binding assay. In this case, there was a dramatic decrease in binding performance (>80%), which was attributed to denaturation of the protein in the presence of the low ionic strength buffer. This was confirmed by incubating the protein in 2 mM ammonium acetate buffer and assaying enzyme activity every hour. As shown in Figure 7B, the protein retained only 20% of its initial activity after this treatment. Taken together, these experiments demonstrate that the use of low ionic strength buffers, which are required for ESI-MS, result in denaturation of DHFR, causing the loss of column performance.

Figure 8 shows the reproducibility between columns within the same batch (i.e., cut from the same capillary). In this case, different 10-cm columns were cut from the midsection of a 1-m-long capillary and were examined after washing 30 bed volumes of buffer through the column over a period of 1 h to remove glycerol and any loosely adsorbed protein. The data are all

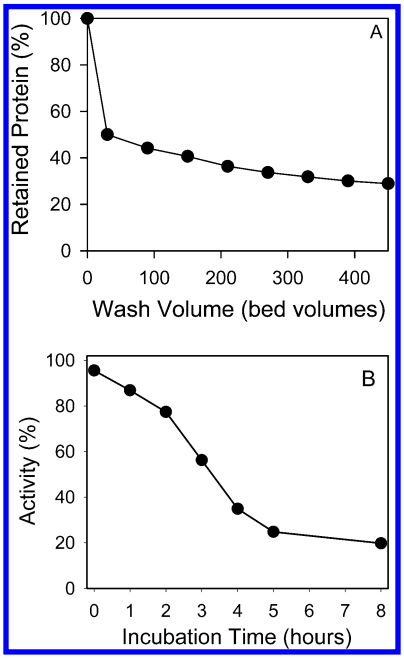

Figure 7. Contributions to loss of column performance due to leaching and denaturation of DHFR. Panel A: amount of fluorescein-labeled DHFR remaining within macroporous monolithic columns after washing 450 bed volumes through the column over 8 h. Panel B: effect of incubation in 2 mM ammonium acetate (used as FAC/MS running buffer) on DHFR activity.

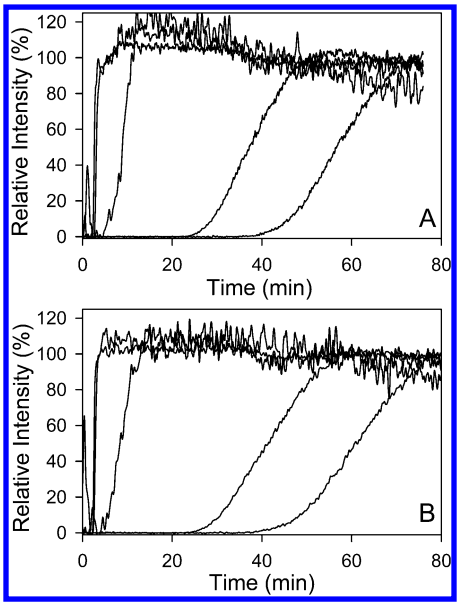

Figure 8. Column-to-column reproducibility for elution of five compounds. Panels A and B show FAC/MS data obtained for two different columns cut from one continuously filled capillary. Columns were infused with a solution containing 20 nM coumarin, folate, trimethoprim, and pyrimethamine and 100 nM fluorescein in 2 mM ammonium acetate. The order of elution was coumarin (2.7 and 2.6 min), fluorescein (3.1 and 2.9 min), folate (8.9 and 8.4 min), trimethoprim (37.2 and 41.4 min), and pyrimethamine (56.7 and 61.4 min).

obtained for the first run of compounds through the columns. It is clear that the columns show acceptable reproducibility, with the relative standard deviation (RSD) between columns being in the range of 5% or less. Reproducibility between columns obtained from different batches was slightly poorer, showing RSD values

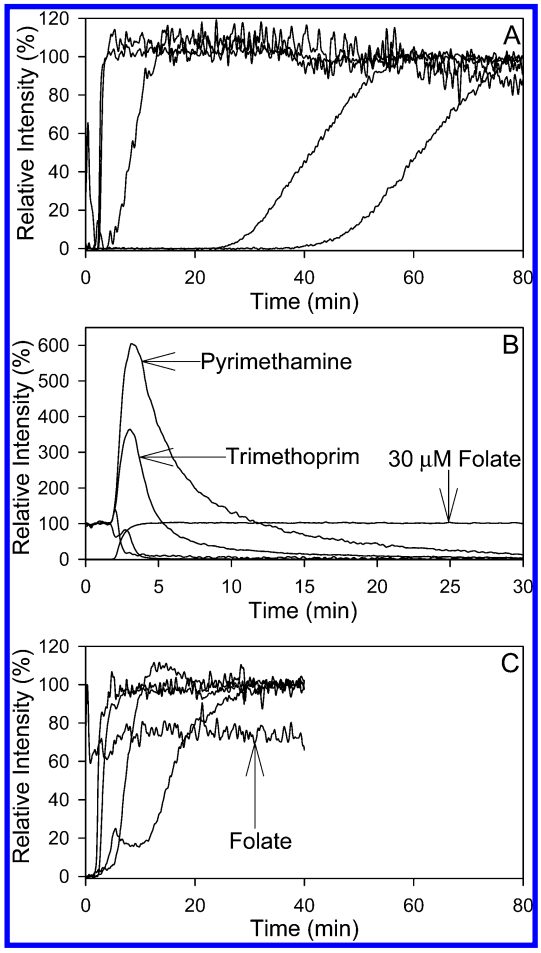

Figure 9. Run-to-run reproducibility and column regeneration for a 5-day-old DGS/PEO/APTES column containing an initial loading of 50 pmol of DHFR. The order of elution for panel A (initial run) was coumarin, fluorescein, folate, trimethoprim, and pyrimethamine. After reequilibrating the column with 2 mM ammonium acetate, 30 mM folate was flowed through the column for 40 min to displace tightly bound affinity analytes in panel B. The column was then reequilibrated with 2 mM ammonium acetate before FAC was repeated in panel C.

on the order of 8% (data not shown). These data suggest that the sol−gel composition and processing methods used to form the column lead to reproducible column performance and make it possible to directly compare data obtained from different columns. This is further supported by the data shown in Figure 6, where data obtained from four different columns was combined to generate reliable K_d and B_t values with $r^2 > 0.998$.

Figure 9 shows the reproducibility between runs (panels A and C) and the regeneration of the columns (panel B) using a weak affinity ligand (folic acid) to displace stronger binding ligands (pyrimethamine and trimethoprim). The displacement of tight-binding ligands by a known weak binder (panel B) can be used to confirm their specificity for the catalytically relevant site on the surface of the target protein. The retention time for pyrimethamine drops from 60 to 15 min while those for trimethoprim drop from 40 to 7 min after column regeneration (panels A and C). Thus, even after washing the column with an excess of a weak ligand to aid in displacement of stronger ligands, the original column activity is not recovered. This is consistent with

the data presented above (Figure 7), which show that prolonged exposure of the entrapped protein to the low ionic strength running buffer leads to irreversible denaturation of the entrapped protein. It is also possible that binding of the strong ligand led to partial irreversible inhibition of the protein.

DISCUSSION

Meso/macroporous sol−gel-based monolithic bioaffinity columns are ideally suited for the screening of compound mixtures using frontal affinity chromatography with mass spectrometric detection for identification of specific compounds in the mixture. The ability to interface the capillary columns directly to an ESI mass spectrometer is a key advantage of the new columns and is likely to make them suitable for HTS of compound mixtures using FAC/MS. While direct comparison to bead-based columns was not done in the present study, the monolithic columns clearly provide advantages in terms of ease of column loading and control over protein loading. Columns were formed simply by mixing the hydrolyzed silane with the polymer and protein-doped buffer and pumping the mixture into the capillary prior to spinodal decomposition and gelation. This one-step column fabrication method leads to good column-to-column reproducibility. The monolithic columns retained up to 25% of the loaded protein in an active form based on the B_t values reported above. The monolithic columns also have low back pressures (due to the macroporous nature of the material), which allows the use of a low-pressure syringe pump for pumping of eluents. The ability to operate at low pressures and low flow rates makes the monolithic columns amenable to direct interfacing with ESI-MS, with no need for flow splitting. This maximizes sensitivity and thus results in an ability to use low levels of compounds and hence small amounts of immobilized protein (∼10 pmol). This latter point is likely to be of significant importance when expensive or low-abundance proteins are used as targets for FAC/MS-based screening. Library compounds may be equally valuable and available in small quantities, making this technique more attractive.

One of the major advances in the development of the new columns was the use of the biocompatible sol−gel precursor DGS for column fabrication. Recent studies from our group have conclusively demonstrated that DGS and related sugar-modified silanes are able to maintain the activity of a wide variety of proteins and, in particular, are able to stabilize proteins that denature readily when entrapped in materials derived from alkoxysilanes such as tetraethyl orthosilicate.[31] The evolution of glycerol as a byproduct of DGS hydrolysis maintains the entrapped proteins in an active state during column aging, yet is readily removed from the column during the initial column flushing step owing to its small size relative to the protein, avoiding elution of glycerol into the mass spectrometer. The ability to remove entrapped glycerol from DGS-derived materials by washing has been previously confirmed by thermogravimetric analysis.[37]

A key issue that was examined as part of column optimization was minimization of nonselective retention mechanisms, which could result from interactions of compounds with the silica matrix. Since silica is polar and anionic, it is expected that interactions with polar and cationic compounds might occur, as was observed in our work. Counterbalancing of the anionic charge using the cationic silane APTES resulted in a remarkable reduction in nonselective retention, while at the same time not producing significant changes in entrapped protein behavior. APTES could be easily incorporated into the column by adding it to a buffered PEO/protein solution, and the level could be adjusted simply by altering the APTES concentration in the starting buffer mixture.

While the monolithic columns provide good chromatographic results, several problems remain to be overcome to optimize column performance. One issue is the leaching of entrapped functional protein (∼70%). Better control over pore morphology may result in the ability to maximize the ratio of mesopores to macropores, leading to retention of a higher fraction of entrapped protein. However, 100% entrapment does not seem feasible, as it would require either removal of macropores or strong protein bonding to the matrix, which is likely to cause significant alterations in protein-binding constants. Another issue is the tendency of DHFR to denature in the low ionic strength running buffer that is required for ESI-MS. While this issue may be of particular significance for DHFR, it is likely that other proteins would also be unstable in such a buffer. This appears to be an inherent drawback of FAC/ESI-MS and not specific to the column format described here. It is possible that coimmobilization of protein-stabilizing groups using novel sol−gel precursors may solve this problem. A final issue with the bioaffinity columns is the inability to regenerate the column. This problem is likely due to denaturation of DHFR in the running buffer, but it should be noted that this issue is ubiquitous in immunoaffinity chromatography[1a] after binding of high-affinity ligands, and useful methods to overcome this problem have not yet been developed. While column regeneration is clearly desirable, this goal will likely require significant efforts to identify conditions that can dissociate bound ligands without irreversibly denaturing the entrapped protein. In all likelihood, these conditions would have to be optimized for each new protein. Fortunately, it is possible to prepare several columns with good reproducibility using a single length of capillary, and thus, it is possible that rather than regenerating columns one could simply use new columns for each run and compare intercolumn runs to obtain B_t or K_d data, if needed.

While the current work has focused on entrapment of a soluble enzyme, the sol−gel method employed herein is also amenable to the entrapment of a wide range of important drug targets, including membrane-bound enzymes and receptors[15] and even whole cells.[42] Furthermore, entrapment into DGS-derived materials allows immobilization of labile enzymes, such as factor Xa and Cox-II, which are difficult to immobilize by other methods.[31] Thus, the monolithic columns may find use in screening of compound mixtures against a wide variety of useful targets.

CONCLUSIONS

Monolithic silica columns containing entrapped proteins are shown to be amenable to bioaffinity-based screening of small molecule−protein interactions using frontal chromatography in conjunction with mass spectrometric detection. The new columns are formed using a biocompatible one-pot processing method involving the addition of a buffered aqueous solution containing PEO (MW 10 000) and the protein of interest to a hydrolyzed solution of DGS, followed by loading of the column. The resulting material retains protein activity and, at the same time, provides

(42) Livage, J.; Coradin, T.; Roux, C. *J. Phys.: Condens. Matter* **2001**, *13*, R673.

the required bimodal pore distribution that is needed to obtain good flow of eluent with low back pressure. Inclusion of a small amount of APTES is shown to reduce nonselective adsorption, resulting in a column that retains compounds primarily as a result of bioaffinity interactions with entrapped proteins. Formation of columns within 150−250-μm-i.d. fused-silica capillaries provides a system that requires only very small amounts of protein (50 pmol loading, 12 pmol of active protein) to produce a useful bioaffinity column. Such columns are suitable for pressure-driven liquid chromatography and can be operated at relatively high flow rates (up to 500 μL·min^{-1}) with low back pressures. More importantly, the operation of these columns with low ionic strength eluents allows direct interfacing to an electrospray mass spectrometer, allowing identification of small molecules using the multiple reaction monitoring mode, although such buffers do lead to relatively rapid denaturation of the entrapped protein. The ability to detect inhibitors present in compound mixtures via retention time combined with MS detection may prove to be very powerful for high-throughput screening of compound mixtures.

ACKNOWLEDGMENT

The authors thank the Natural Sciences and Engineering Research Council of Canada, MDS-Sciex, the Canadian Foundation for Innovation, and the Ontario Innovation Trust for financial support of this work. The authors also thank Dr. Eric Brown of the Department of Biochemistry at McMaster University for providing DHFR, and Russ Gill and Dr. Matthias Thommes of Quantachrome Inc. for obtaining mercury intrusion porosimetry data. M.A.B. thanks the Canada Council for the Arts for providing a Killam Fellowship. J.D.B. holds the Canada Research Chair in Bioanalytical Chemistry.

Received for review October 14, 2003. Accepted March 4, 2004.

AC0352124